scientific reports

Check for updates

OPEN

5-HMF inhibits glucocorticoid-induced osteoporosis through the VEGFR2/PI3K/AKT pathway

Siqi Liu[1], Fei Fang[2]✉ & Yu Jiang[1]✉

Chronic administration of glucocorticoids are being linked to an increased risk of osteoporosis. 5-Hydroxymethylfurfural (5-HMF) is a natural compound that possesses various biological activities, including osteogenic regulation. In this research, we sought to investigate the potential of 5-HMF to exert protective effects against glucocorticoid-induced osteoporosis. In cellular investigations, we deployed Western Blot (WB), Real-Time Quantitative real-time PCR (qRT-PCR), Alkaline phosphatase (ALP) and Alizarin S-red (ARS) staining to scrutinize the expression of osteogenic differentiation markers within MC3T3-E1 pre-osteoblasts and BMSCs. We used dexamethasone to establish a mouse model for glucocorticoid-Induced osteoporosis and administered 5-HMF to evaluate its influence on bone density and architecture through the use of micro-CT and histological analysis. In addition, we employed network pharmacology to elucidate the potential pathways and targets of 5-HMF. Finally, we explored the effect of AKT knockout on the treatment of 5-HMF. We found that 5-HMF significantly enhanced VEGFR2 phosphorylation, reestablishing angiogenesis and activating the PI3K/AKT pathway in vitro and in vivo. 5-HMF also inhibited Dexamethasone -induced apoptosis by regulating Bax and Bcl-2 expression. MK2206, an AKT inhibitor, abrogated 5-HMF's protective properties against GCs. These results indicate that 5-HMF counteracts the negative effects of GCs on osteoblasts and has good bone-promoting differentiation effects.

Keywords Dexamethasone, 5-Hydroxymethylfurfural, VEGFR2/PI3K/AKT signaling, Osteoblast differentiation, Glucocorticoid-Induced osteoporosis

Glucocorticoids (GCs) play a key role in the treatment of a variety of autoimmune and inflammatory diseases as anti-inflammatory and immunosuppressive agents[1]. The effects of GCs on bones have also attracted a lot of attention. The process of osteogenic differentiation is contingent upon Glucocorticoids[2]. Emerging research has underscored the negative impact of GCs on osteoblasts (OBs), including suppression of their survival[3], differentiation capabilities[4], and induction of apoptosis[5], which is proposed as a cardinal mechanism driving GCs-induced bone loss. However, there is currently a lack of specific treatment strategies for GCs-induced osteoporosis. Given the paucity of targeted therapeutic approaches for GIOP, it is of great clinical significance to explore the pathogenesis and find effective prevention and treatment strategies.

5-Hydroxymethylfurfural (5-HMF), a bioactive compound emerging from the realms of food processing and traditional Chinese medicine, has recently garnered significant attention for its biomedical potential, which encompasses antioxidant[6], anti-ischemic[7] and anti-inflammatory activities[8]. Extensive research has demonstrated the positive impacts of 5-HMF on a myriad of conditions, including anti-osteoporotic effects, antioxidant properties, wound healing promotion, and immune system modulation[9–12]. However, whether and how 5-HMF acts in GIOP chemotherapy resistance remains to be fully elucidated.

VEGFR2 and its downstream signaling cascade, the phosphatidylinositol 3-kinase (PI3K)/protein kinase B (AKT) pathway, play a central role in GIOP, which regulates bone angiogenesis[13,14], cell survival[15], the functional regulation of osteoblasts and osteoclasts[16] and bone remodeling[17], lead to increase of osteoclast activity. However, the activation state of the PI3K/AKT pathway is intricately linked to the balance between bone formation and resorption[18]. When phosphorylated at the 407th site, AKT activates downstream BMP2, which then directs RUNX2 to exert its nuclear transcriptional function, regulating cellular osteogenic signaling pathways[19]. In addition, Bcl-2 is downstream of the PI3K/AKT signaling pathway and is closely related to the negative regulation of apoptosis[20]. Bcl-2 depolymerizes with phosphorylated BAD, and free Bcl-2 can block the release of cytochrome C from mitochondria and prevent the activation of caspase apoptotic proteins[21], exerting anti-apoptotic effects. Therefore, we hypothesized that 5-HMF has a potential impact on the occurrence and

[1]Jiangnan University Medical Center, Wuxi 214001, PR China. [2]Wuxi School of Medicine, Jiangnan University, Wuxi 214100, China. ✉email: 8202212004@jiangnan.edu.cn; jiangyu@jiangnan.edu.cn

progression of GIOP, ultimately by modulating the VEGFR2/PI3K/AKT signaling pathway to alleviate DEX-induced osteogenic inhibition and apoptosis.

In this work, we aimed to investigate the contribution of 5-HMF and VEGFR2/PI3K/AKT signaling in long-term glucocorticoid-induced bone remodeling. We aim to elucidate the underlying mechanisms of 5-HMF and explore novel therapeutic strategies for the management of glucocorticoid-related bone diseases.

Result

The impact of 5-HMF and DEX on BMSC proliferation and osteogenic differentiation

To ascertain the effects of 5-HMF and DEX on the proliferation of BMSCs and MC3T3-E1 cells, which both possess osteogenic differentiation capabilities, we treated the cells with a basal medium containing 10% FBS, supplemented with a gradient of concentrations of 5-HMF and DEX. Following a 48-hour incubation, the proliferation of the cells was quantified using the CCK-8 assay (Fig. 1A, D). Then, the mineralization capacity of both cells was assessed with ALP staining at 0, 7, and 10 days (SI-Figure 1). Our results revealed that 100 μM DEX significantly impaired the osteogenic capacity of BMSCs and MC3T3-E1 during the differentiation process (Fig.1B-C), and 5-HMF promoted osteogenic differentiation at low to medium concentrations (0.1-10 μM) (Fig. 1E-F).

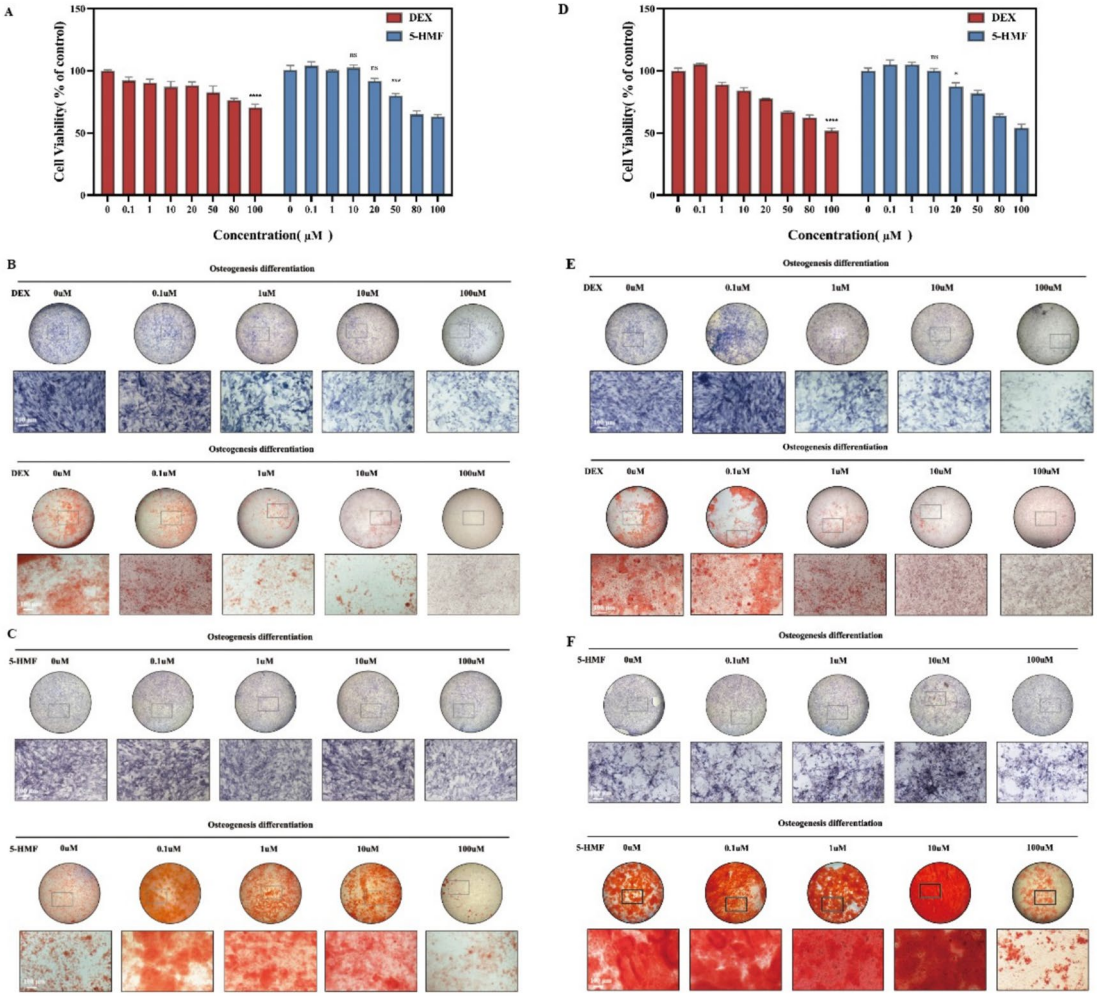

Fig. 1. Osteogenic differentiation potential of two cell lines. **A**. CCK8 shows the toxicity and side effects of DEX and 5-HMF on BMSCs cell lines at different concentration gradients. **B**-**C**. The results of ALP staining and ARS staining indicated the effects of different concentration gradients of DEX and 5-HMF on the osteogenic differentiation of BMSCs. **D**. CCK8 shows the toxicity and side effects of DEX and 5-HMF on MC3T3-E1 cell lines at different concentration gradients. **E**-**F**. The results of ALP staining and ARS staining indicated the effects of different concentration gradients of DEX and 5-HMF on the osteogenic differentiation of MC3T3-E1. Stained images were respectively acquired at 4X and 10X magnification. Data are presented as mean ± SEM of at least three independent experiments. Statistical significance was determined by one-way ANOVA followed by Dunnett's post-hoc test (or Student's t-test, if only two groups). *$p < 0.05$, **$p < 0.01$, **$p < 0.001$ versus the control group.

5-HMF treatment inhibits GC-induced bone differentiation in vitro

Based on the aforementioned findings, we selected 100 μM DEX as the induction concentration for subsequent in vitro GIOP models and employed a combination treatment of 5-HMF and DEX to observe the effects of 5-HMF on DEX-induced osteogenic and mineralization defects in BMSCs. Staining with alkaline phosphatase and Alizarin Red confirmed that treatment with 5-HMF effectively mitigated the osteogenic and mineralization defects caused by DEX (Figure 2A-D). Concurrently, during BMSC osteogenic differentiation, 5-HMF treatment elevated the mRNA and protein expression levels of osteogenic markers in BMSCs, without affecting the inherent osteogenic processes of the cells when treated alone (Figure 2F-G). These results indicate that 5-HMF can promote osteogenic differentiation in vitro, even in the presence of glucocorticoids. The results of immunofluorescence also confirmed this conclusion (Figure 2H-J).

5-HMF administration elicits an increase in bone in vivo

To further validate the osteogenic effects of 5-HMF, we examined its efficacy in a mouse model of GIOP. A GIOP mouse model was established with continuous DEX administration for 90 days, and 5-HMF was orally administered to counteract the severe bone loss (Figure 3A). Compared with Dex group, 5-HMF significantly protected mice against bone loss, demonstrated by reduced daily body weight loss (Figure 3B). To preliminarily assess the safety profile of 5-HMF in the disease context, we examined histopathology (H&E staining) and organ indices of the liver, thymus, and kidney. Compared to the GIOP (Dex-only) group, co-administration of 5-HMF did not exacerbate tissue damage or alter organ weights, suggesting that 5-HMF is well-tolerated within this glucocorticoid-induced osteoporotic model (Figure 3C-D). Micro-CT scans were utilized to assess DEX-induced osteoporosis in mice, quantifying the reduction in bone volume fraction, trabecular thickness,

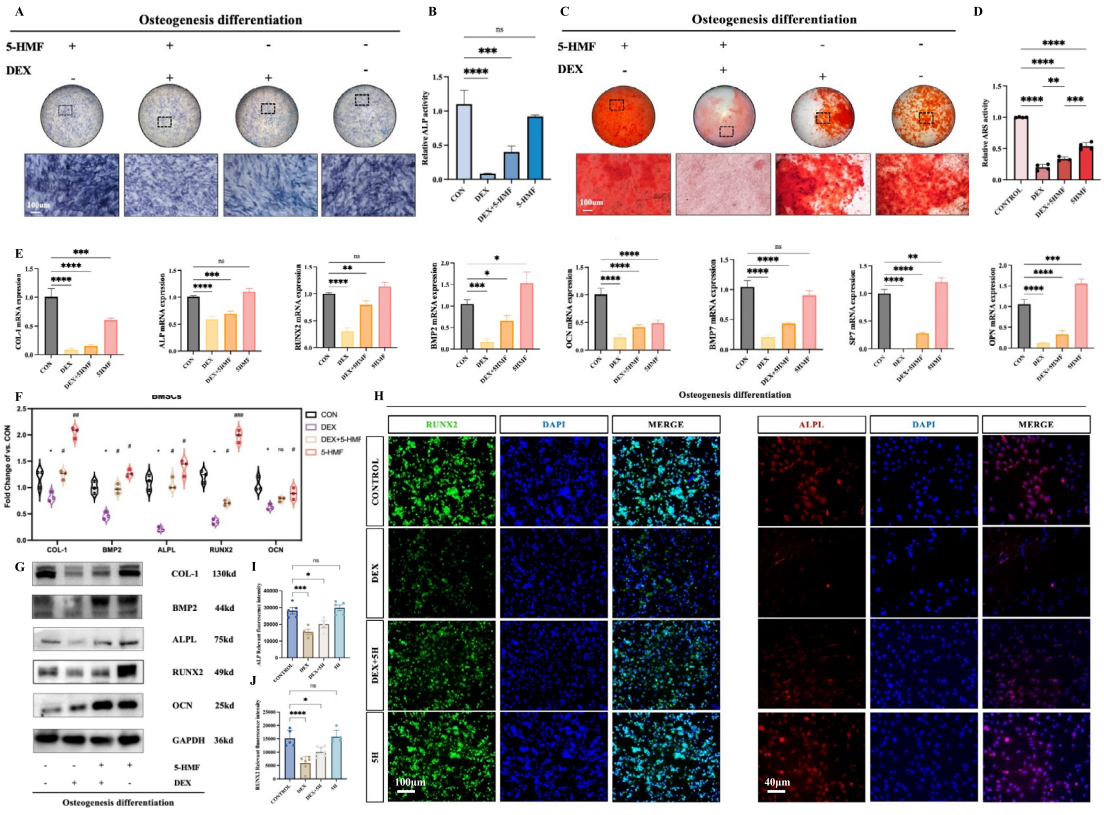

Fig. 2. 5-HMF treatment inhibits GC-induced bone differentiation in vivo. **A**. Representative ALP staining images of BMSCs after 14 days of treatment (10× view). **B**. Quantification of relative ALP activity. **ns, not significant; *p < 0.05, **p < 0.01 vs. control group. **C**. Representative ARS staining images of BMSCs after 14 days of treatment (10× view). **D**. Quantification of relative ARS activity. **ns, not significant; *p < 0.05, **p < 0.01 vs. control group. **E**. Q-PCR quantification of osteogenic markers in BMSCs cells. **F-G**. Relative expressions of COL-1, BMP2, ALPL, RUNX2, and CON were determined by Western blot. In panel F, asterisks (*) indicate statistical significance compared to the CON group, while hash marks (#) indicate statistical significance compared to the DEX group. **H-J**. Representative IF images and quantification showing the expression and localization of RUNX2 (10× magnification) and ALPL (20× magnification) in BMSCs after 14 days of treatment. Data are presented as mean ± SD from three independent experiments. One-way ANOVA and Tukey's multiple comparison test were performed on the data from the experiment between the four groups: *p < 0.05; **p < 0.01; ***p < 0.001; ****p < 0.0001. Cells were treated with 10 μM 5-HMF、100 μM DEX for 14 Days.

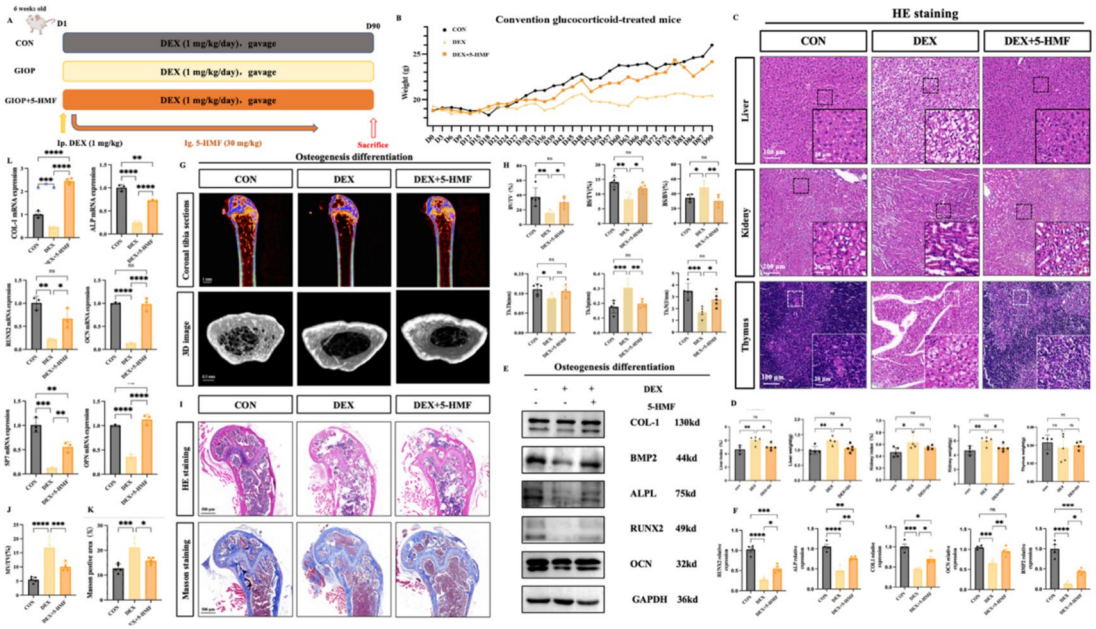

Fig. 3. 5-HMF administration elicits an increase in bone in vivo. **A**. Schematic diagram of 5-HMF treatment. Dex (1 mg/kg) was administered to SPF C57BL/6J mice by intraperitoneal injection. Then 5-HMF (30mg/kg) was gavaged every day. **B**. The change in daily body weight of mice within 3 months after Dex injection. **C**. HE staining of liver, kidney, and thymus of mice in each group. **D**. Wet weights and index of liver, kidney, and thymus in each group (Stained images were respectively acquired at 10X and 20X magnification). **E-F**. Relative expressions of COL-1, BMP2, ALPL, RUNX2, and CON were determined by Western blot. **G**. 2D and 3D images of micro-CT in each group of mice. **H**. Quantification of BV/TV, BS/TV, BS/BV, Tb.Th, Tb.Sp and Tb.N in mice in each group. **I**. HE staining, and Masson staining show bone tissue morphology in each group of mice. **J-K**. HE and Masson staining semi-quantitative results show bone tissue morphology in each group of mice. **L**. qPCR quantification of relevant osteogenic markers in bone tissue of mice in each group. One-way ANOVA and Tukey's multiple comparison test were performed on the data from the experiment between groups: *p < 0.05; **p < 0.01; ***p < 0.001; ****p < 0.0001. Data are presented as mean ± SD (n=5 mice per group).

and trabecular number (Figure 3G-H). Histological analysis with H&E and Masson's trichrome staining of bone tissues also confirmed that 5-HMF treatment restored the reduction in trabecular density caused by DEX, compared to DEX alone (Figure 3I-K). The mRNA and protein expression levels of osteogenic markers further substantiated this observation (Figure 3E-F, L).

5-HMF alleviated DEX-induced osteoporosis via the VEGFR2/PI3K/Akt axis

To elucidate the potential signaling pathways underlying the osteoprotective effect of 5-HMF, we first employed a network pharmacology approach. Potential targets of 5-HMF were retrieved from the TCMSP and TCMID databases. Disease targets for glucocorticoid-induced osteoporosis (GIOP) were collected from GeneCards, OMIM, PharmGkb, and DrugBank databases. Venn analysis identified 20 overlapping target genes between 5-HMF and GIOP, suggesting their involvement in the therapeutic mechanism (Fig. 4A). Subsequent KEGG pathway enrichment analysis of these intersecting genes revealed that the VEGF signaling pathway was the most significantly enriched, with the VEGFR2 node playing a central role (Fig. 4B). Since VEGFR2 is a key regulator of angiogenesis, which is coupled with osteogenesis, we next evaluated the effect of 5-HMF on endothelial cell function in vitro. Using human umbilical vein endothelial cells (HUVECs), we found that 5-HMF treatment significantly enhanced cell migration in a scratch wound healing assay and promoted the formation of capillary-like structures in a tube formation assay, compared to the DEX-treated group (Fig. 4C, D). Quantitative analysis confirmed these pro-angiogenic effects (Fig. 4E). We then investigated whether 5-HMF modulates the VEGFR2 pathway and its downstream effector, the PI3K/AKT axis, in osteoblast-lineage cells. Western blot analysis of bone marrow mesenchymal stem cells (BMSCs) showed that DEX treatment markedly reduced the phosphorylation levels of VEGFR2 and AKT, as well as the expression of total VEGFR2, PI3K, and AKT. Co-treatment with 5-HMF effectively restored the expression and activation of these key pathway components (Fig. 4F, G, L, M). Consistent with the cellular findings, immunohistochemistry (IHC) staining of mouse femoral bone sections demonstrated that 5-HMF administration rescued the DEX-induced downregulation of VEGFR2, PI3K, and AKT protein levels in vivo (Fig. 4H, I). Furthermore, immunocytochemistry (ICC) in BMSC-derived models confirmed the enhanced phosphorylation of VEGFR2, PI3K, and AKT upon 5-HMF treatment (Fig. 4J, K).

Collectively, these data indicate that 5-HMF mitigates glucocorticoid-induced osteogenic impairment by activating the VEGFR2/PI3K/AKT signaling axis, which may involve promoting associated angiogenic processes.

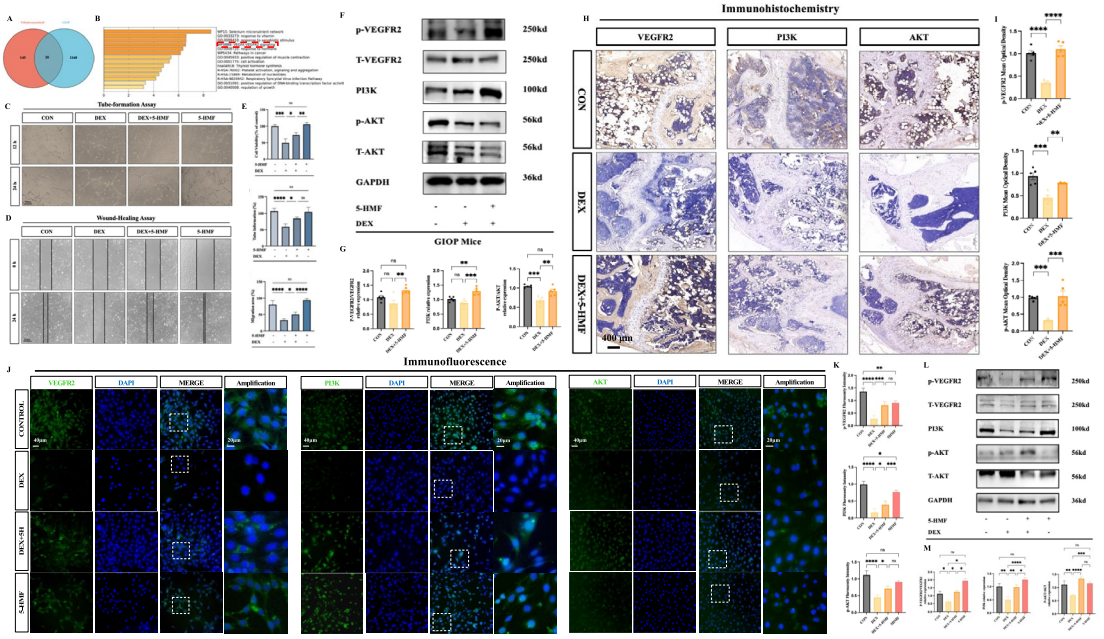

Fig. 4. 5-HMF alleviated DEX-induced osteoporosis by promotting the VEGFR2/PI3K/Akt axis. **A**. Intersection of target targets of 5-HMF and DEX. **B**. KEGG pathway Enrichment in intersection targets. **C-D**. Representative images of HUVEC cell scratch wound healing assay and tube formation assay (images acquired at 4× magnification). **E**. Quantitative results of the scratch wound healing assay, tube formation assay, and CCK-8 assay. **F-G**. Representative Western blot images (**F**) and quantification (**G**) of p-VEGFR2, VEGFR2, p-PI3K, PI3K, p-Akt, and Akt expression in BMSCs. **H-I**. Representative IHC images **(J)** and quantification (**K**) of VEGFR2, PI3K, and AKT expression in bone tissue sections (images acquired at 5× magnification). **J-K**. Representative ICC images (**H**) and quantification (**I**) of p-VEGFR2, p-PI3K, and p-Akt in BMSC-derived small intestinal organoids (images acquired at 20× and 40× magnification). **L-M**. Representative Western blot bands (**L**) and quantification (**M**) of p-VEGFR2, VEGFR2, p-PI3K, PI3K, p-Akt, and Akt in BMSCs. Cell-based data are presented as mean ± SD from three independent experiments. Mouse data are presented as mean ± SD (n=5 mice per group).

Akt inhibitor eliminated the therapeutic effect of 5-HMF on Dex-induced osteoporosis

To further confirm whether 5-HMF alleviated Dex-induced osteoporosis by modulating the VEGFR2/PI3K/Akt axis, we administered MK2206 (an inhibitor of Akt) into both BMSCs and MC3T3-E1 in in vitro experiments. For the inhibition assay, cells were treated with 100 μM Dexamethasone, co-treated with 10 μM 5-HMF, and further combined with 10 μM MK2206 for the entire 14-day differentiation period. The results of ALP and ARS staining showed that the addition of MK2206 to 5-HMF treatment attenuated the bone-contributing effect of 5-HMF (Fig. 5A-F). The mRNA expression level of osteogenic markers was recalled after MK2206 use as shown by Real-time PCR (Figure 5J-K). The WB results further confirmed that the protine expression levels of ALP, BMP2, COL1A1, OCN, RUNX2, Akt and p-Akt were significantly down-regulated under MK2206 treatment (Figure 5L-O), which was consistent with the IF results (Figure 5 G-I). These results show that Akt inhibitors can eliminate the therapeutic effect of 5-HMF on Dex-induced osteoporosis.

Inhibiting AKT expression restored the apoptotic phenotype

Through TUNEL staining, immunofluorescence, Real-time PCR and Western blotting, we discovered that high concentrations of Dex induce apoptosis in BMSCs and MC3T3-E1 cells, while the administration of 5-HMF counteracts this apoptotic effect of Dex (Fig. 6). To further probe the role of 5-HMF in Dex-induced apoptosis of osteoblasts and MC3T3-E1 cells, MK2206—an AKT-specific inhibitor—was co-administered with 5-HMF and Dex in these cells. As depicted in Fig. 6D-I, the addition of MK2206 significantly abrogated the anti-apoptotic effects of 5-HMF in BMSCs and MC3T3-E1 cells (Fig. 6)

Discussion

Although several therapeutic agents are currently employed in the treatment of GIOP, including risedronic acid, alendronic acid, teriparatide, and denosumab, a significant therapeutic gap persists[22–24]. Consequently, the development of drugs capable of effectively reversing Dex-induced osteoporosis is of urgent importance, holding substantial significance for improving patient outcomes associated with bone loss due to glucocorticoid therapy. Previous reports revealed low concentrations of 5-HMF can augment bone formation by stimulating the proliferation and differentiation of osteoblasts both in vitro and in vivo[9,25]. However, it is unclear whether and how 5-HMF is effective in GIOP. This study verified the alleviating effect of 5-HMF on glucocorticoid-induced bone damage, and revealed the possible pathways of action. Utilizing network pharmacology, we identified the

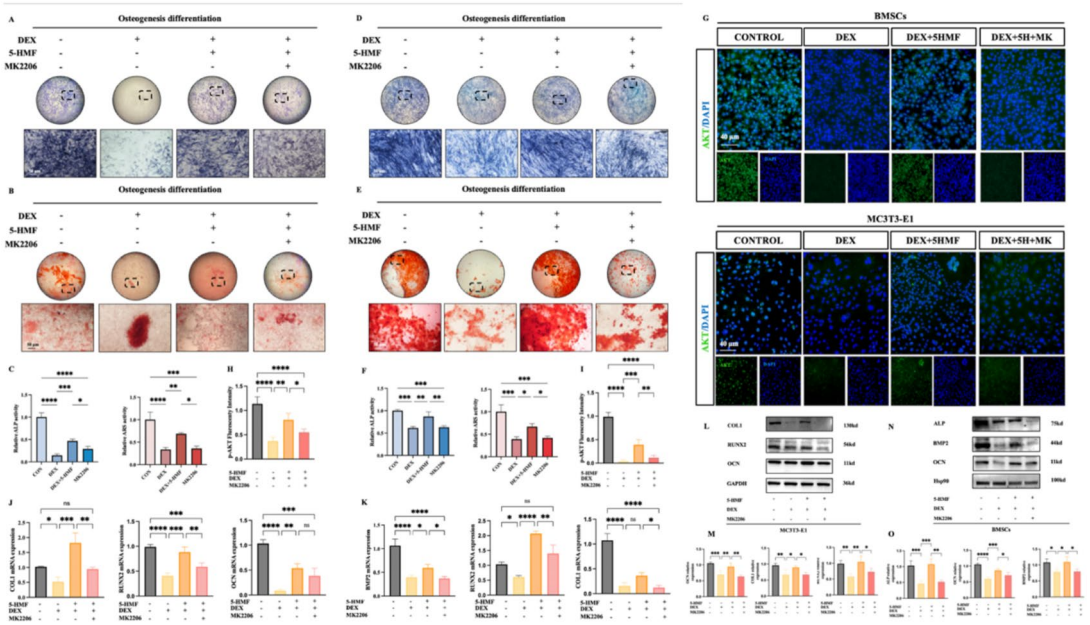

Fig. 5. Akt inhibitor eliminated the therapeutic effect of 5-HMF on Dex-induced osteoporosis. **A**-**B**.ALP staining and ARS staining results for no treatment, DEX treatment, DEX co-treatment with 5-HMF, and in the presence of MK 2206 in BMSCs. **C**. the relative expression of ALP staining and ARS staining both in BMSCs. **D**-**E**.ALP staining and ARS staining results for no treatment, DEX treatment, DEX co-treatment with 5-HMF, and in the presence of MK 2206 in MC3T3-E1. **F**. the relative expression of ALP staining and ARS staining both in MC3T3-E1. **G**. Representative IF images of p-AKT in BMSCs and MC3T3-E1 (Stained images were respectively acquired at 20X magnification). **H**-**I**. Quantification of p-AKT immunofluorescence signal intensity in BMSCs (**H**) and MC3T3-E1 cells (**I**). **J**-**K**. Quantitative reverse transcription polymerase chain reaction (qRT-PCR) analysis of key osteogenic marker genes in BMSCs (**J**) and MC3T3-E1 cells (**K**) under the indicated treatments. **L**-**M**. Western blot analysis of osteogenic markers in MC3T3-E1 cells. Representative blots (**L**) and their densitometric quantification (**M**) are shown. **N**-**O**. Western blot analysis of the same panel of proteins in BMSCs. Representative blots (**N**) and their densitometric quantification (**O**) are shown. Data in bar graphs are presented as the mean ± standard deviation (SD) from three independent experiments. Statistical significance was determined by one-way ANOVA followed by Tukey's post hoc test. Significance levels: *p < 0.05, **p < 0.01, ***p < 0.001, ****p < 0.0001. Treatment groups: CON (untreated control), DEX (10 μM dexamethasone), DEX+5-HMF (DEX + 10 μM 5-HMF), DEX+5-HMF+MK (DEX + 10 μM 5-HMF + 10 μM MK-2206). All in vitro treatments were administered for 14 days under osteogenic induction conditions.

VEGF-VEGFR2 pathway, which play a central role in endothelial cell survival[26], proliferation, migration, and lumen formation[27,28]. Therefore, HUVECs were used to decipher the effects of 5-hydroxymethylfurfural. The results indicated that 5-HMF group promotes HUVECs migration, proliferation and demonstrated a significant increase in the number of HSECs tube formation, compared to the Dex induced group.

Our study also explores how 5-HMF activates the downstream pathway of VEGFR2 to target bone metabolism. To date, a direct link between VEGFR2 and bone remodeling has not been definitively established. However, the engagement of VEGFR2 triggers a cascade of intracellular signaling pathways, which encompass the activation of key signaling molecules such as p38, ERK1/2, PI3K/Akt, and Src/FAK[29,30]. Ma et al.[31] have indicated that the proliferation and differentiation of rat osteoblasts require the activation of the PI3K/AKT signaling pathway, which is partially regulated by BMP2 molecules. BMPs promote osteogenesis, osteoclastogenesis, and chondrogenesis at all differentiation stages[32]. The intricate dialogue between VEGFR2 and the PI3K/AKT signaling network raises the intriguing possibility that this VEGFR2-PI3K-AKT axis is instrumental in the regulatory mechanisms mediated by 5-HMF. The results proved that 5-HMF administration restored the phosphorylation of VEGFR2 and AKT proteins inhibited by DEX, and promoted the expression of classical osteogenic transcription factors BMP2 and RUNX2. The high enrichment of the PI3K/AKT signaling pathway indicates its key role in 5-HMF-induced osteogenic differentiation. These findings confirmed our hypothesis that 5-HMF regulates VEGFR2 function by modulating phosphokinase activity, while actively regulating the activity of key osteogenic factors through its downstream PI3K/Akt signaling pathway, further promoting osteoblast differentiation.

Meanwhile, the function of inhibiting DEX-induced apoptosis was detected on 5-HMF. Zhang et al. have reported that Dex inhibits angiogenic processes and can lead to avascular osteonecrosis of the femoral head[33]. The results of this study showed that 5-HMF was effective in attenuating DEX-induced apoptosis both in vivo and in vitro. Notably, the use of an AKT inhibitor attenuates the osteogenic inhibition of 5-HMF on DEX actions, while restoring the apoptotic phenotype. The result underscores the central role of the AKT in the modulation of DEX-induced bone remodeling and cell apoptosis by 5-HMF (Fig. 7).

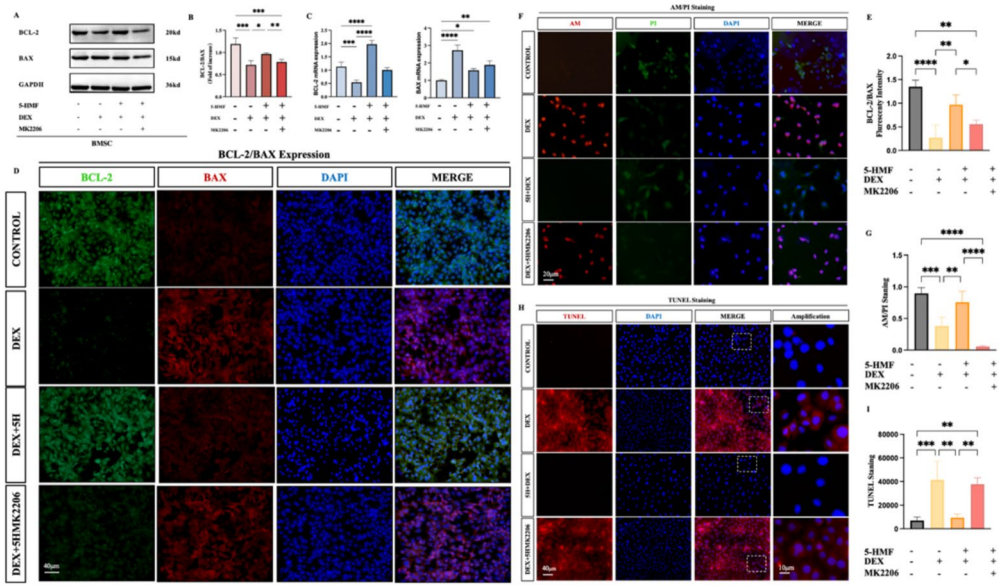

Fig. 6. Inhibiting AKT expression restored the apoptotic phenotype. **A**-**B**. The relative expression and the relative density analysis results of Bcl-2 and Bax were determined by Western blot in BMSCs. **C**. qPCR quantification of Bcl-2 and Bax in BMSCs. **D**. Representative IF images of Bcl-2 and Bax in MC3T3-E1 (Stained images were respectively acquired at 20X magnification). **E**. Representative IF images of AM/PI staining in MC3T3-E1 (Stained images were respectively acquired at 40X magnification). **F**. Representative IF images of TUNEL staining in BMSCs (Stained images were respectively acquired at 20X magnification). Data in bar graphs are presented as the mean ± standard deviation (SD) from three independent experiments. Statistical significance was determined by one-way ANOVA followed by Tukey's post hoc test. Significance levels: *p < 0.05, **p < 0.01, ***p < 0.001, ****p < 0.0001. Treatment groups: CON (untreated control), DEX (10 μM dexamethasone), DEX+5-HMF (DEX + 10 μM 5-HMF), DEX+5-HMF+MK (DEX + 10 μM 5-HMF + 10 μM MK-2206).

Furthermore, our research has revealed that chronic glucocorticoid administration leads to steatosis in the livers of mice, and the administration of 5-HMF alleviated this pathological change in the liver. Recent studies have suggested that bone is the endocrine organ of the human body, and the metabolites secreted by it affect other organs in our body[34].A finding underscored by literature[35] indicated an inseparable link between the bone and liver circulating osteocalcin levels, which are thought to be associated with hepatic fat infiltration. Our study suggests that 5-HMF may help reduce glucocorticoid-induced intrahepatic fat accumulation. However, it remains unclear whether this effect is linked to bone metabolism or represents an independent mechanism unrelated to bone metabolism, necessitating further investigation. Collectively, our findings underscore the potential of 5-HMF in modulating VEGFR2/PI3K/AKT signaling pathways that are critical for maintaining bone health and countering the effects of glucocorticoid-induced osteoporosis. These findings not only provide a new perspective for understanding the mechanism of action of 5-HMF in the regulation of glucocorticoid-induced osteoblastic differentiation dysfunction, but also provide a new therapeutic strategy for the development of glucocorticoid-associated osteoporosis.

Materials and methods

Ethical approval

For all the experiments, 6-week-old age C57BL/6J wild-type littermate controls were used. The C57BL/6J mice were provided by Gem Pharmatech, China. The animals were housed in a specific pathogen-free animal facility certified by Wuxi Medical College in Jiangsu, China. Mice are housed at a temperature of 20-26 °C and 40-70% relative humidity in a 12-hour circadian cycle with unrestricted access to water and food. Experimental/control mice in each litter are co-housed in individually ventilated cages on the same rack in the animal facility. All animal procedures followed the guidelines set forth by the Ethics Committee for Medical Animal Experiments in Wuxi, Jiangsu, China (Jiangsu, China, permit number: SYXK(Su)2021-0056, permit number: JN.No 20221120T0180415). All animal experiments were performed according to the ARRIVE guidelines.

Experimental animals and bone staining

Fifteen female C57 mouses (20-25 g, 6-week-old) were randomly divided into three groups: Control, GIOP, GIOP+5-HMF (n = 5 in each group) and housed in standard temperature conditions with a 12-h light/dark cycle. The mice were housed in transparent plastic cages and allowed ad libitum access to normal chow diet and water. Repeat experiments with at least three different sample sets were planned and the numbers of animals required were determined accordingly. The establishment of GIOP model was according to previous studies[36], receiving an intramuscular injection of dexamethasone (1 mg/kg/day in 0.9% NaCl solution) for 90 days, while

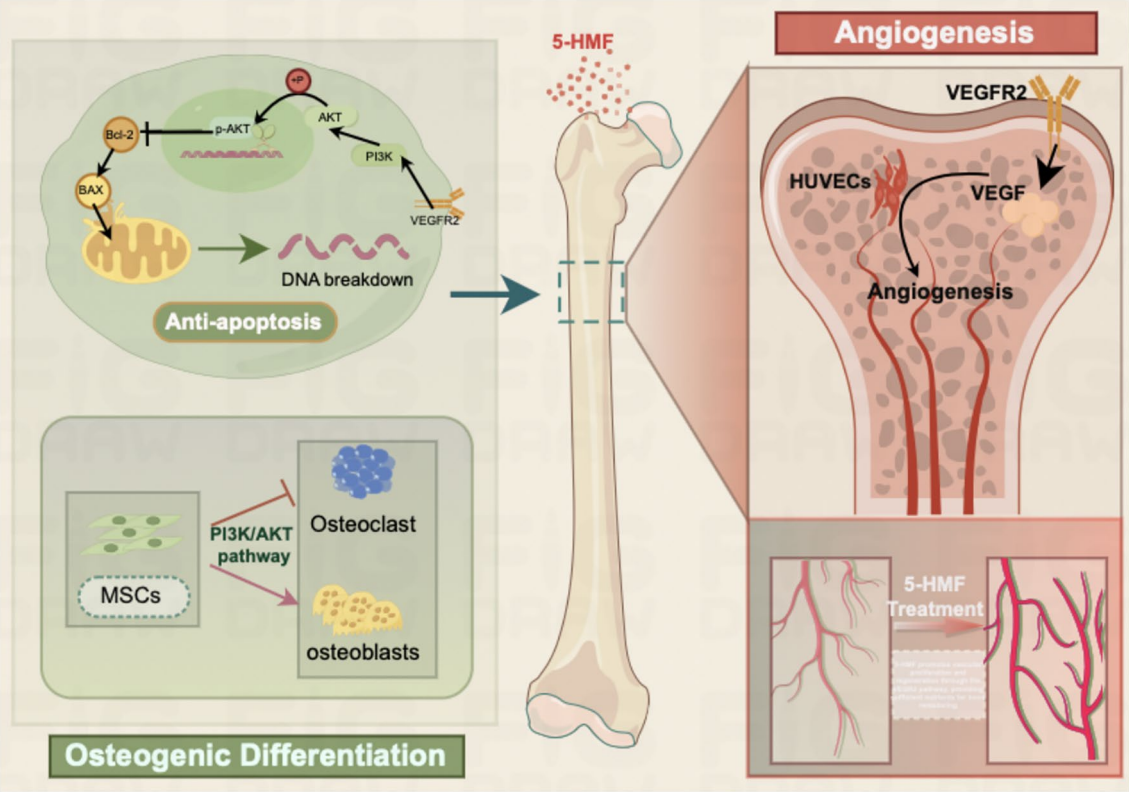

Fig. 7. Mechanism of action diagram of 5-HMF in the treatment of GIOP. 5-HMF regulates osteogenesis through the VEGFR2/PI3K/AKT pathway, inhibits cell apoptosis, and treats DEX-induced osteoporosis. Created by Figdraw.

a control group was injected daily with equal volume vehicle (saline). At the same time, the treatment group is given intragastric administration of 5-HMF (30 mg/kg/day in 0.9% NaCl solution) once a day. In contrast, the Dex groups received equal volume PBS treatment only.

To monitor dynamic bone formation and mineralization, at the end of the treatment period, these mouses were exposed to 1.8% isoflurane for 2-3 minutes of anesthesia, followed by eye blood collection, supplemented by cervical dislocation and sacrifice. Then, the right femurs were used for protein and RNA extraction, while the left femurs were decalcified in 4% FPA for micro-CT scanning. Post-micro-CT analysis, the femurs were harvested and decalcified using 10% EDTA for a period of thirty days, prior to staining with hematoxylin and eosin (H&E), Masson's trichrome (Masson's Trichrome Stain Kit, G1343, Beijing Solarbio Science & Technology Co., Ltd.), and subjecting them to immunohistochemistry and immunofluorescence analyses. It is noted that the investigators did not maintain blindness to allocation during the experimental procedures and outcome assessments. Sample sizes were determined based on precedent experiments, and no animals were excluded from the analysis.

Micro-CT scanning

Micro-CT scanning and corresponding analysis for femurs were performed using SkyScan1178 system and bundled software (Bruker MicroCT, Kontich, Belgium). 2D and 3D reconstructions were performed using DataViewer and CTVox software respectively. The region of interest (ROI) was selected as the trabecular bone at the metaphyseal region of the distal femur, located inferior to the growth plate. Quantitative assessments of bone mineral density (BMD), trabecular bone volume fraction (BV/TV), trabecular number (Tb.N), trabecular thickness (Tb.Th), and trabecular separation (Tb.Sp) were performed utilizing CTAn software.

Cell culture and processing

BMSCs, MC3T3-E1 and HUVECs cells from the Servies biotechnology Cell Bank (Servies, Wuxi, CN) were grown at 37 °C in DMEM medium supplemented with 10 % FBS (Excell Bio, Shanghai, CN) and 1 % penicillin/streptomycin (Biosharp, Anhui, CN). In the course of this experiment, BMSCs, MC3T3-E1 and HUVECs cells were subjected to a treatment with 100 μM Dex and 10 μM 5-HMF (Aladdin Biochem Technology, Shanghai, China) for a period of 7-21 days. The osteogenic media was induced using DMEM containing 10% FBS, 1% PS, 10 mM β-glycero phosphate disodium salt hydrate and 300 μM ascorbic acid.

Tube formation assay

Briefly, cold Matrigel (Cat#211212, NEST Biotechnology, CN) was used to coat the 24-well plate. Next, the plates were incubated at 37°C for 4 hours, and then human umbilical vein endothelial cells (1×10^4cells/well) in 1000 μL conditioned medium, were seeded to Matrigel-coated wells and incubated for 12 to 24 hours at 37°C. A microscope was used to observe the formation of capillary-like structures. Image J software version 1.52 (NIH, Bethesda, MD) was used to assess branching points formed by endothelial cells per image field. Here and later, data were graphed as means ± SD for experiments performed three times, each in triplicate.

Cell viability assay

BMSCs and MC3T3-E1 cells (a density of 2×10^3 cells/well) were seeded on a 96-well culture plate.BMSCs and MC3T3-E1 cells viability test was carried out by Cell Counting Kit-8 (CCK8, Abbkine, Wuhan,China). Briefly, cells were added to 96-well plates at a density of 2× 103 cells/mL and treated with DEX, 5-HMF (0, 0.1, 1, 10, 20, 50, 100 μM) for 48h. Next, 10 μL of CCK8 solution was added,and the cells were incubated for 30 min. The cell viability was measured by assessing the optical density at a wavelength of 450 nm using a microplate reader.

Alkaline phosphatase (ALP) and Alizarin S-red (ARS) activity assay

BMSCs and MC3T3-E1 cells (a density of 1×10^4 cells/well) were seeded on a 48-well culture plate and cultured by osteogenic media. At 7, 14 and 21days, the cell-seeded samples were washed twice with PBS (pH 7.4), fixed for 10 min using 3.7% formaldehyde and washed with PBS again. All of the samples were stained using 300ul Alizarin S-red staining solution (pH 4.2) and BCIP/NBT solution (Biosharp, Anhui, CN), incubated at 37 °C for 1 h. The staining solution was removed after 1 h, the cells were washed with distilled water three times. ARS-stained mineralization was quantified by dissolving the stain in 10% cetylpyridinium chloride and measuring the absorbance at 570 nm, with results normalized to the control group.

Real-time polymerase chain reaction (real-time PCR)

According to manufacturer's instructions, 1 μg of total RNA was extracted from all samples and transcribed into cDNA. Real-time PCR amplifications on all samples were carried out by RT-PCR SYBR Green RT Premix (Yeasen, Shanghai, CN). The primers of the measured mRNA genes were as shown in Table 1. The relative expression was normalized to GAPDH employing the $2^{-\Delta\Delta Ct}$ method.

Western blotting analysis

For protein analysis related to osteogenic differentiation, cells were treated with the indicated compounds (e.g., Dex, 5-HMF, MK2206) under osteogenic induction conditions for 14 Days to lysis. The protein content in both cells and bone tissue was determined using the BCA method (CWBIO, Beijing, China). SDS–PAGE (sodium dodecyl sulfate–polyacrylamide gel electrophoresis) was used for electrophoresis of the samples, and the separated proteins were transferred to polyvinylidene fluoride (PVDF) membranes. Briefly, after electrophoresis and transfer, PVDF membranes were cut into strips prior to antibody incubation to optimize the use of primary

Gene ID	Sequence (5' to 3')	Length of the product (bp)
GAPDH	F: TGTGTCCGTCGTGGATCTGA	20
	R: CCTGCTTCACCACCTTCTTGAT	22
BMP2	F: ATGTGAGGATTAGCAGGTCTTTG	23
	R: TCGTTTGTGGAGCGGATGT	19
RUNX2	F: GCCAATCCCTAAGTGTGGCT	20
	R: AACAGAGAGCGAGGGGGTAT	20
ALP	F: AGACCAGGTCTGCTCAGGAT	20
	R: ACCCCGCTATTCCAAACAGG	20
SP7	F: CGCATCTGAAAGCCCACTTG	20
	R: CAGCTCGTCAGAGCGAGTGAA	21
OPN	F: CTGGCAGCTCAGAGGAGAAG	20
	R: CAGCATTCTGTGGCGCAAG	19
COL1A1	F: GCTCCTCTTAGGGGCCACT	19
	R: CCACGTCTCACCATTGGGG	19
BMP7	F: AGGAGTAATCGCAAGCCTCG	20
	R: TTTGAGGCCACATCCCTCAC	20
OCN	F: TGGGCCTCCATATGACCTCGAGTAG	25
	R: TCAAAGGCTTGTAAATTGGAGGAGT	25
Bcl-2	F: AGCATGCGACCTCTGTTTGA	20
	R: GCCACACGTTTCTTGGCAAT	20
BAX	F: AGGCCTCCTCTCCTACTTCG	20
	R: CCTTTCCCCTTCCCCCATTC	20

Table 1. Sequences of the primers for quantitative RT-PCR analyses.

	Antibody	Dilution Factor	Corporation	Catlog
Primary antibody	GAPDH	1:1000	Proteintech	10494-1-AP
	BMP2	1:1000	Wanleibio	WLH3885
	RUNX2	1:1000	Zen-bioscience	380494
	ALP	1:1000	Zen-bioscience	381009
	COL1A1	1:1000	MCE	HY-P81227
	OCN	1:1000	Zen-bioscience	614487
	Bcl-2	1:1000	HUABIO	HA723111
	BAX	1:1000	UpingBioHANGZHOU.CHINA	YP-Ab-00125
	P-AKT	1:1000	Proteintech	80455-1
	AKT	1:1000	Zen-bioscience	342529
	p-VEGFR2	1:1000	Zen-bioscience	310186
	VEGFR2	1:1000	Bosterbio	A00901-3
	PI3K	1:1000	Bosterbio	R380934

Table 2. The primary antibodies used in immunoblotting analyses.

antibodies. Each strip was incubated with a specific primary antibody against the target protein. Due to standard laboratory workflow, images of the intact, uncut membranes were not captured prior to this step. Instead, all original, unprocessed images of the individual membrane strips (including complete membrane edges and molecular weight markers) are provided in the Supplementary Information file (SI-wb.pdf). For illustrative clarity, a schematic representation of the full-length membrane, assembled from the individual strips, is also included. All Western blot experiments were performed in triplicate, and representative images are shown in the main figures.

The membranes were preincubated with a blocking buffer (obtained from Shanghai, China) for a duration of 1 hour, followed by an overnight incubation at 4 °C with a suitably diluted primary antibody (1:1000, Zen-bioscience, CN). Subsequently, the secondary antibodies used were goat anti-rabbit and anti-mouse IgG conjugated with horseradish peroxidase (HRP) at 1:10000 and the protein was visualized with enhanced chemiluminescence reagent (Cat#abs920, Absin, Shanghai, CN). Signals are detected and analyzed using a luminescence image analyzer. The main antibodies used can be found in Table 2.

Immunofluorescence

BMSCs and MC3T3-E1 cells (50 % confluency) were cultured in 24-well plates for 3days under different treatment conditions. The plates were slowly rinsed to fix and seal cells and incubated overnight at 4 °C in the dark with Primary antibodies (1:100, Upingbio, HANGZHOU, CN). After washing with PBS, they were incubated with the secondary antibody in the dark for 2 h and labeled with DyLight 594 and DyLight 480 fluorescent probes (Thermo, UK). The DAPI-stained nuclei were observed using a fluorescence microscope (Olympus, Tokyo, Japan). The AM/PI apoptosis staining kit was obtained from Elabscience Biotechnology Co., Ltd. (Wuhan, China).

Network pharmacology

To more comprehensively collect and organize information on 5-HMF and their targets, three web-based pharmacological databases were searched: TCMSP (https://tcmsp-e.com/), TCMID database (https://bidd.group/TCMID/) and Swiss TargetPrediction database (http://swisstargctprediction.ch/). The data of 5-HMF and their targets from the aforementioned databases were collated, and after merging and de-duplication, standardized gene names of 5-HMF-related targets were obtained using the UniProt database (https://www.uniprot.org/).

Four databases were used to retrieve data on angiogenesis-related disease targets, including the GeneCards database (http://www.genecards.org/), DrugBank database (https://go.drugbank.com/), OMIM database (https:/www.ncbi.nlm.nih.gov/omim/), and PharmGkb database (https://www.pharmgkb.org/), and they were searched using "GIOP, glucocorticoid-induced osteoporosis" as a keyword. Then, using the Excel spreadsheet function, the target data from the three aforementioned databases were combined, and after merging and de-duplication, standardized gene names were obtained using the UniProt database. Next, the obtained GIOP-related targets were compared with 5-HMF targets to obtain crossover targets of angiogenesis and 5-HMF.

Animal sacrifice

Mice were anesthetized with 1.8% isoflurane for 2–3 minutes. All anesthetized animals were sacrificed by cervical dislocation, and successful death was confirmed by the absence of vital signs.

Statistical analysis

Data are presented as mean ± SD. For comparisons among three or more groups, one-way ANOVA was performed, followed by Dunnett's post-hoc test (for comparison vs. a single control) or Tukey's post-hoc test (for all pairwise comparisons), as appropriate. The specific test used for each experiment is indicated in the corresponding figure legend. A p-value < 0.05 was considered statistically significant.

Conclusion

Collectively, this study elucidates that 5-HMF exerts protective effects against glucocorticoid-induced osteoporosis primarily through activating the VEGFR2/PI3K/AKT signaling axis. This activation promotes osteogenic differentiation and suppresses apoptosis in osteoblasts. These findings not only offer a novel perspective on the role of 5-HMF in modulating glucocorticoid-induced osteoblast dysfunction but also pave the way for developing new therapeutic strategies targeting glucocorticoid-associated osteoporosis

Data availablility

The raw data supporting the conclusions of this article will be made available by the authors, without undue reservation. All data generated or analysed during this study are included in this published article (and its Supplementary Information files). If any questions need to be consulted, the data supporting this study's findings are available from the corresponding author upon reasonable request. Data is provided within the supplementary information files.

Received: 9 February 2025; Accepted: 11 March 2026
Published online: 18 March 2026

References

1. Auger, J. P. et al. Metabolic rewiring promotes anti-inflammatory effects of glucocorticoids. *Nature* **629**, 184–192. https://doi.org/10.1038/s41586-024-07282-7 (2024).
2. Glynn, E. R., Londono, A. S., Zinn, S. A., Hoagland, T. A. & Govoni, K. E. Culture conditions for equine bone marrow mesenchymal stem cells and expression of key transcription factors during their differentiation into osteoblasts. *J. Anim. Sci. Biotechnol.* **4**, 40. https://doi.org/10.1186/2049-1891-4-40 (2013).
3. Li, H. Z. et al. Role of signaling pathways in age-related orthopedic diseases: Focus on the fibroblast growth factor family. *Mil. Med. Res.* **11**, 40. https://doi.org/10.1186/s40779-024-00544-5 (2024).
4. Zheng, X. et al. Delay the progression of glucocorticoid-induced osteoporosis: Fraxin targets ferroptosis via the Nrf2/GPX4 pathway. *Phytother. Res.* **38**, 5203–5224. https://doi.org/10.1002/ptr.8310 (2024).
5. Jiang, H. et al. Taxifolin-mediated Nrf2 activation ameliorates oxidative stress and apoptosis for the treatment of glucocorticoid-induced osteonecrosis of the femoral head. *Phytother. Res.* **38**, 156–173. https://doi.org/10.1002/ptr.8031 (2024).
6. Zhao, L. et al. In vitro antioxidant and antiproliferative activities of 5-hydroxymethylfurfural. *J. Agric. Food Chem.* **61**, 10604–10611. https://doi.org/10.1021/jf403098y (2013).
7. Pagare, P. P. et al. The antisickling agent, 5-hydroxymethyl-2-furfural: Other potential pharmacological applications. *Med. Res. Rev.* **44**, 2707–2729. https://doi.org/10.1002/med.22062 (2024).
8. Ziadlou, R. et al. Regulation of inflammatory response in human osteoarthritic chondrocytes by novel herbal small molecules. *Int. J. Mol. Sci.* https://doi.org/10.3390/ijms20225745 (2019).
9. Tan, X. L. et al. 5-(Hydroxymethyl)-2-furaldehyde inhibits adipogenic and enhances osteogenic differentiation of rat bone mesenchymal stem cells. *Nat. Prod. Commun.* **9**, 529–532 (2014).
10. Yalcin, O. & Cabrales, P. Increased hemoglobin O2 affinity protects during acute hypoxia. *Am. J. Physiol. Heart Circ. Physiol.* **303**, H271-281. https://doi.org/10.1152/ajpheart.00078.2012 (2012).
11. Kong, F., Fan, C., Yang, Y., Lee, B. H. & Wei, K. 5-hydroxymethylfurfural-embedded poly (vinyl alcohol)/sodium alginate hybrid hydrogels accelerate wound healing. *Int. J. Biol. Macromol.* **138**, 933–949. https://doi.org/10.1016/j.ijbiomac.2019.07.152 (2019).
12. Zhang, H. et al. 5-Hydroxymethylfurfural alleviates inflammatory lung injury by inhibiting endoplasmic reticulum stress and NLRP3 inflammasome activation. *Front. Cell Dev. Biol.* **9**, 782427. https://doi.org/10.3389/fcell.2021.782427 (2021).
13. Lee, K. S. et al. Inhibition of VEGF blocks TGF-beta1 production through a PI3K/Akt signalling pathway. *Eur. Respir. J.* **31**, 523–531. https://doi.org/10.1183/09031936.00125007 (2008).
14. Zhou, C., Hu, G., Li, Y. & Zheng, S. Polydatin accelerates osteoporotic bone repair by inducing the osteogenesis-angiogenesis coupling of bone marrow mesenchymal stem cells via the PI3K/AKT/GSK-3beta/beta-catenin pathway. *Int. J. Surg.* https://doi.org/10.1097/JS9.0000000000002075 (2024).
15. Baek, J. Y., Kwak, J. E. & Ahn, M. R. Eriocitrin inhibits angiogenesis by targeting VEGFR2-mediated PI3K/AKT/mTOR signaling pathways. *Nutrients* https://doi.org/10.3390/nu16071091 (2024).
16. Lauzon, M. A., Drevelle, O., Daviau, A. & Faucheux, N. Effects of BMP-9 and BMP-2 on the PI3K/Akt pathway in MC3T3-E1 preosteoblasts. *Tissue Eng. Part A* **22**, 1075–1085. https://doi.org/10.1089/ten.TEA.2016.0151 (2016).
17. Andreasen, C. M. et al. Local coordination between intracortical bone remodeling and vascular development in human juvenile bone. *Bone* **173**, 116787. https://doi.org/10.1016/j.bone.2023.116787 (2023).
18. Sun, K. et al. The PI3K/AKT/mTOR signaling pathway in osteoarthritis: a narrative review. *Osteoarthr. Cartil.* **28**, 400–409. https://doi.org/10.1016/j.joca.2020.02.027 (2020).
19. Cohen-Solal, K. A., Boregowda, R. K. & Lasfar, A. RUNX2 and the PI3K/AKT axis reciprocal activation as a driving force for tumor progression. *Mol. Cancer* **14**, 137. https://doi.org/10.1186/s12943-015-0404-3 (2015).
20. Hers, I., Vincent, E. E. & Tavare, J. M. Akt signalling in health and disease. *Cell. Signal.* **23**, 1515–1527. https://doi.org/10.1016/j.cellsig.2011.05.004 (2011).
21. Chen, Q., Ray, S., Hussein, M. A., Srkalovic, G. & Almasan, A. Role of Apo2L/TRAIL and Bcl-2-family proteins in apoptosis of multiple myeloma. *Leuk. Lymphoma* **44**, 1209–1214. https://doi.org/10.1080/1042819031000068052 (2003).
22. Ding, H. et al. Dexamethasone-induced apoptosis of osteocytic and osteoblastic cells is mediated by TAK1 activation. *Biochem. Biophys. Res. Commun.* **460**, 157–163. https://doi.org/10.1016/j.bbrc.2015.02.161 (2015).
23. Chiodini, I., Merlotti, D., Falchetti, A. & Gennari, L. Treatment options for glucocorticoid-induced osteoporosis. *Expert Opin. Pharmacother.* **21**, 721–732. https://doi.org/10.1080/14656566.2020.1721467 (2020).
24. Rice, J. B., White, A. G., Scarpati, L. M., Wan, G. & Nelson, W. W. Long-term systemic corticosteroid exposure: a systematic literature review. *Clin. Ther.* **39**, 2216–2229. https://doi.org/10.1016/j.clinthera.2017.09.011 (2017).
25. Jiang, Y., Zhong, Z., Wang, M. & Zhang, X. 5-Hydroxymethyl-2-furaldehyde induces developmental toxicology and decreases bone mineralization in zebrafish larvae. *Comp. Biochem. Physiol. C Toxicol. Pharmacol.* **254**, 109254. https://doi.org/10.1016/j.cbpc.2021.109254 (2022).
26. Sawamiphak, S. et al. Ephrin-B2 regulates VEGFR2 function in developmental and tumour angiogenesis. *Nature* **465**, 487–491. https://doi.org/10.1038/nature08995 (2010).
27. Koch, S. & Claesson-Welsh, L. Signal transduction by vascular endothelial growth factor receptors. *Cold Spring Harb. Perspect. Med.* **2**, a006502. https://doi.org/10.1101/cshperspect.a006502 (2012).
28. Kofler, N. M. & Simons, M. Angiogenesis versus arteriogenesis: neuropilin 1 modulation of VEGF signaling. *F1000Prime Rep.* **7**, 26. https://doi.org/10.12703/P7-26 (2015).

29. Tan, P. et al. PI3K/AKT/mTOR signaling regulates BCP ceramic-induced osteogenesis. *J. Mater. Chem. B.* **12**, 7591–7603. https://doi.org/10.1039/d4tb01335b (2024).
30. Zhao, T. L. et al. 5-methoxytryptophan induced apoptosis and PI3K/Akt/FoxO3a phosphorylation in colorectal cancer. *World J. Gastroenterol.* **29**, 6148–6160. https://doi.org/10.3748/wjg.v29.i47.6148 (2023).
31. Ma, P. et al. Glimepiride induces proliferation and differentiation of rat osteoblasts via the PI3-kinase/Akt pathway. *Metabolism* **59**, 359–366. https://doi.org/10.1016/j.metabol.2009.08.003 (2010).
32. Banerjee, C. et al. Differential regulation of the two principal Runx2/Cbfa1 n-terminal isoforms in response to bone morphogenetic protein-2 during development of the osteoblast phenotype. *Endocrinology* **142**, 4026–4039. https://doi.org/10.1210/endo.142.9.8367 (2001).
33. Zhang, X. X. et al. Bone marrow mesenchymal stem cells overexpressing HIF-1α prevented the progression of glucocorticoid-induced avascular osteonecrosis of femoral heads in mice. *Cell Transplant.* **31**, 9636897221082687. https://doi.org/10.1177/09636897221082687 (2022).
34. Fernandez-Real, J. M. et al. Circulating osteocalcin concentrations are associated with parameters of liver fat infiltration and increase in parallel to decreased liver enzymes after weight loss. *Osteoporos. Int.* **21**, 2101–2107. https://doi.org/10.1007/s00198-010-1174-9 (2010).
35. Hodgson, S. F. et al. Bone loss and reduced osteoblast function in primary biliary cirrhosis. *Ann. Intern. Med.* **103**, 855–860. https://doi.org/10.7326/0003-4819-103-6-855 (1985).
36. Zha, X. et al. Regulatory effect of microRNA-34a on osteogenesis and angiogenesis in glucocorticoid-induced osteonecrosis of the femoral head. *J. Orthop. Res.* **36**, 417–424. https://doi.org/10.1002/jor.23613 (2018).

Author contributions

Yu Jiang and Fei Fang conceived and designed the study. Siqi Liu wrote the manuscript, translated the manuscript, made manuscript revisions. All authors have read and approved the manuscript.

Funding

This study was supported by Double-Hundred Talent Personnel Project of Wuxi Health Committee (BJ2023041) and Research Project of the Health Commission of Jiangsu Province (Z2022027).

Declarations

Competing interests

The authors declare no competing interests.

Ethics approval

Animal procedures followed the regulations of the animal care committee, which were approved by the Institutional Animal Care and Use Committee of Jiangnan University, approval number JN.No 20221120t0180415, and the experiments were performed in accordance with the approved guidelines and regulations. The experiments complied with the ARRIVE guidelines.

Additional information

Supplementary Information The online version contains supplementary material available at https://doi.org/10.1038/s41598-026-44463-y.

Correspondence and requests for materials should be addressed to F.F. or Y.J.